Comparison of Processing Power System Events using Time-Frequency Analysis and Adaptive Comb Filters

[1]S. Deepa and [2]P. Vanaja Ranjan

*[1]Research Scholar, [2]Associate Professor,
Department of Electrical and Electronics Engineering,
College of Engineering Guindy Campus, Anna University, Chennai, India
E-mail: deepasundaresan@yahoo.com, vranjanau@yahoo.co.in*

Abstract

Power quality of electric power system has become an increasing concern for electric utilities and their customers over the last decade. The goal of monitoring non-stationary signal is to quantify the dynamic nature of these signals and to extract the important features that support the integrated monitoring system that can be used in maintenance scheduling and system operation. The paper discusses the use of different time-frequency domain methods for power system disturbance analysis. The use of time-frequency analysis method is difficult to accurately detect all power system events by single method. The adaptive notch filter has been used for the power signal event detection. This method gives best performances than the time-frequency analysis.

Index Terms: Adaptive comb filters, power system events/disturbances, event detection.

Introduction

Power system signals are often polluted and distorted by undesired components as a result of nonlinear loads mainly power-electronic devices. Harmonics are spectral components at frequencies that are integer multiples of the ac signals fundamental frequency. Interharmonics are spectral components at frequencies that are not integer multiples of the system fundamental frequency. Besides the typical problems caused by harmonics such as overheating and useful life reduction, the interharmonics also create some new problems, such as subsynchronous oscillations, voltage fluctuations,

and light flicker, even for low-amplitude levels. Interharmonics can be observed in an increasing number of loads in addition to harmonics. These loads include static frequency converters, adjustable speed drives for induction or synchronous motors, arc furnaces, and certain loads that are not pulsating synchronous with the fundamental power system frequency as discussed in [1-3]. The presence of interharmonic components strongly increases difficulties in modeling and measuring the distorted waveforms. This is mainly due to the variability of the waveform periodicity, the variability of their frequencies and amplitudes and the great sensitivity to the spectral leakage phenomenon.

A signal detection algorithm requires accurate and real time measurement of individual harmonic and interharmonics within a signal and their signal attributes, such as magnitudes, phase angles and frequencies. Mutual erroneous impacts of harmonics/interharmonic components on each other, their dynamic nature, and the noise are the challenging factors in power system events, thereby rendering it an active field of research. A variety of techniques exists and used to analyze harmonics which has been discussed in [4-5]. In order to overcome these difficulties proper signal detection algorithm requires for accurate and real time measurement of individual harmonic within a signal and their signal attributes, such as magnitudes, phase angles and frequencies. Most of the methods for signal analysis are based on the use of the Fourier transform (FT) [6], which breaks down a signal into constituent sinusoids of different frequencies. The Fourier analysis transforms the signal from a time-based or space based domain to a frequency-based one. Unfortunately, in transforming to the frequency domain, the time or space information is limited, as it is impossible to determine when or where a particular event took place [7]. To overcome this deficiency a new technique, named as short time Fourier Transform (STFT), was proposed by Dennis Gabor [8]. This windowing technique analyzes only a small section of the signal at a time. The STFT maps a signal into a 2-D function of time or space and frequency which helps in studying the variation of various frequency components with time. But STFT suffers from several pitfalls including aliasing, the time window effect, the picket fence, bandwidth localization tradeoff along with other window constraints which reduces the effectiveness of STFT in analysis of non stationary signals. The linear time-frequency representation, wavelet transform has been used for transient detection and harmonic signal decomposition, in which the different frequency signals are not shown in order. The selection of sampling frequency and the mother wavelet is of greater importance [9-13]. A number of algorithms, e.g., least-square techniques [14-19], Kalman filtering [20], Parseval's relation and energy concept [21], adaptive infinite impulse response line enhancer [22], and artificial neural networks [23], have been proposed to extract and measure harmonics under time-varying conditions. Although each exhibits specific advantages, none is reported to demonstrate good performance in frequency-varying environments while having a simple and robust structure suitable for practical applications. The adaptive comb filters are of good choice compared to other methods, whose applications on parameter estimation, harmonic and interharmonic decomposition and harmonic cancellation are important as discussed as in [24-38].

Selective harmonic cancellation has become of primary importance in a wide range of power electronics applications, for example, uninterrupted power systems, regenerative converters, and active power filters. In such applications, the primary objectives are an accurate cancellation of selected harmonics and a quick speed of response under transients. Recently Enhanced Phase Locked Loop (EPLL) [34-36] and Adaptive Notch Filter (ANF) [29] algorithms are proposed in the literature which allows the particular band of frequencies to pass through, therefore it can be called as *Adaptive comb-peak filter (APF)*. These algorithms are more effective in the harmonics estimation and decomposition. In this paper a detailed analysis of these two methods is carried out. This paper is organized as follows: Section II gives a formal definition and statement for the problem encountered in power system through power quality disturbances. Section III discusses on Time-Frequency analysis methods. The detailed analysis of Adaptive comb filters in section IV, results and performance analysis are discussed in Section V with conclusion in Section VI.

Power quality disturbances

Power quality disturbances have been organized into seven categories based on wave shape as transients, interruptions, sag or under voltage, swell or overvoltage, waveform distortion, voltage fluctuations, frequency variations.

1. Transients are potentially the most damaging type of power disturbance, transients fall into two subcategories namely impulsive and oscillatory. Impulsive transients are sudden high peak events that raise the voltage and/or current levels in either a positive or a negative direction. Impulsive transients can be very fast events (5 nanoseconds [ns] rise time from steady state to the peak of the impulse) of short-term duration (less than 50 ns). Causes of impulsive transients include lightning, poor grounding, the switching of inductive loads, utility fault clearing, and ESD (Electrostatic Discharge). The results can range from the loss (or corruption) of data, to physical damage of equipment, of these causes, lightning is probably the most damaging. An oscillatory transient is a sudden change in the steady-state condition of a signal's voltage, current, or both, at both the positive and negative signal limits, oscillating at the natural system frequency. These transients occur when an inductive or capacitive load, such as a motor or capacitor bank is turned off. An oscillatory transient results because the load resists the change.

2. Interruptions: An interruption is defined as the complete loss of supply voltage or load current. Depending on its duration, an interruption is categorized as instantaneous (0.5 to 30 cycles), momentary (30 cycles to 2 seconds), temporary (2 seconds to 2 minutes), or sustained (greater than 2 minutes).

3. Sag/Under voltage: sag is a reduction of AC voltage at a given frequency for the duration of 0.5 cycles to 1 minute's time. Sags are usually caused by system faults and switching loads on with heavy startup currents. Common causes of sags include starting large loads (starting of a large air conditioning unit) and remote fault clearing performed by utility equipment.

4. Swell/Over voltage: A swell is the reverse form of sag, having an increase in

AC voltage for duration of 0.5 cycles to 1 minute's time. The sources of swells are high-impedance neutral connections, sudden (especially large) load reductions, and a single-phase fault on a three-phase system. The result can be data errors, flickering of lights, degradation of electrical contacts, semiconductor damage in electronics, and insulation degradation.

5. Waveform distortion: there are five primary types of waveform distortion namely DC offset, harmonics, interharmonics, notching and noise.

6. Voltage Fluctuations: Since, voltage fluctuations, fundamentally different from the rest of the waveform anomalies, they are placed in their own category. A voltage fluctuation is a systematic variation of the voltage waveform or a series of random voltage changes, of small dimensions, namely 95 to 105% of nominal at a low frequency, generally below 25 Hz. Any load exhibiting significant current variations can cause voltage fluctuations. Arc furnaces are the most common cause of voltage fluctuation on the transmission and distribution system. One symptom of this problem is flickering of incandescent lamps.

7. Frequency Variation: Frequency variation is extremely rare in stable utility power systems, especially systems interconnected via a power grid. The sites having dedicated standby generators or poor power infrastructure, frequency variation is more common especially if the generator is heavily loaded. The most affected are the motor devices or sensitive device that relies on steady regular cycling of power over time.

Time-Frequency Analysis Methods

The frequency content of a signal localized in time is of interest in many applications in which the signal parameters (frequency content etc.) evolve over time. These signals are called non-stationary. The standard Fourier Transform is not suitable for analyzing the nonstationary signal. Information which is localized in time such as spikes and high frequency bursts cannot be easily detected from the Fourier Transform.

Time-frequency localization can be achieved by first windowing the signal to cut a well localized slice and then taking its Fourier Transform. This gives rise to the Short Time Fourier Transform, (STFT) or Windowed Fourier Transform. The magnitude of the STFT is called the spectrogram.

Spectrogram

The time localization can be obtained by suitably pre-windowing the signal, as the FT (spectrum) does not show the time localization of frequency components explicitly. The spectrogram is a time-frequency distribution based on the FT of the product of a sliding window $h(t)$ with the signal. It is given by the following expression for a signal $x(t)$ is

$$S_x(t,f) = \left| \int_{-\infty}^{+\infty} x(\tau) h^*(\tau - t) e^{-j2\pi f\tau} d\tau \right|^2 \tag{1}$$

where $t' = \tau$. The length of the sliding window $h^*(t)$ determines time and frequency resolution, i.e., a good frequency resolution needs a long observation window and therefore leads to a bad localization in time and vice versa. The window length has to be chosen based on the prior knowledge of the signal.

Gabor spectrogram
The Gabor transform is a special case of the STFT. It is used to determine the sinusoidal frequency and phase content of local sections of a signal as it changes over time. The function to be transformed is first multiplied by a Gaussian function, which can be regarded as a window, and the resulting function is then transformed with a Fourier Transform to derive the time-frequency analysis. The Gabor transform for a signal $x(t)$ is

$$G_x(t,f) = \int_{-\infty}^{+\infty} e^{-\frac{1}{2}\left(\frac{\tau-t}{\sigma}\right)^2} e^{-j2\pi f\tau} x(\tau) d\tau \tag{2}$$

Wigner-Ville Distribution
WVD is a quadratic joint TF distribution, which offers a high TF resolution. Given a time signal $x(t)$, WVD is defined by

$$W(t,\omega) = \frac{1}{2\pi} \int_{-\infty}^{\infty} z\left(t+\frac{\tau}{2}\right) z^*\left(t-\frac{\tau}{2}\right) e^{-j\omega\tau} d\tau \tag{3}$$

where $z(t)$ is the analytic signal corresponding to $x(t)$ and $z^*(t)$ is the complex conjugate of $z(t)$.

WVD possesses a great number of good properties, and it has wide interest for fault detection with nonstationary signal analysis. The WVD method suffers from cross-term interference, if the analyzed signal contains more than one frequency component, due to its quadratic nature, resulting in a difficult way of discriminating the actual frequency components.

Choi william distribution
Choi Williams distribution function is one of the members of cohen's class distribution function. This distribution function adopts exponential kernel to suppress the cross-terms. The kernel gain doesnot decrease along the η, τ axes in the ambiguity function. The kernel function of choi-williams distribution can only filter out the cross terms result from the components differs in both time and frequency center.

The definition of the cone-shape distribution function is

$$C_x(t,f) = \int_{-\infty}^{\infty}\int_{-\infty}^{\infty} A_x(\eta,\tau)\phi(\eta,\tau)e^{j2\pi(\eta t-\tau f)} d\eta d\tau \tag{4}$$

where

$$A_x\left(\eta,\tau\right)=\int_{-\infty}^{\infty}x\left(t+\frac{\tau}{2}\right)x^*\left(t-\frac{\tau}{2}\right)e^{-j2\pi t\eta}dt \tag{5}$$

and the kernel function is

$$\phi(\eta,\tau)=e^{-\alpha(\eta\tau)^2} \tag{6}$$

Following are the magnitude distribution of the kernel function in η,τ domain with different α values. The kernel function indeed suppress the interference which is away from the origin, but for the cross-term locates on the η and τ axes, this kernel function can do nothing about it.

Adaptive spectrogram

The adaptive spectrogram method is similar to the gabor spectrogram method. The difference is that the adaptive spectrogram uses the adaptive expansion to decompose the signal and the Gabor spectrogram uses the Gabor expansion to decompose the signal before applying the WVD. The adaptive spectrogram sums only the WVD of the elementary functions, or autoterms, and ignores the crossterms between every two elementary functions. The adaptive spectrogram has a fine and adaptive time-frequency resolution because the elementary functions of the adaptive expansion have a fine and adaptive time frequency resolution with respect to the signal characteristics. The adaptive spectrogram does not include cross-term interference, because it ignores all the crossterms.

Processing of harmonics and interharmonics using APF

Let $r(t)$ Denotes a measured (or computed) signal

$$r(t) = A_1 \sin\varphi_1(t) + \sum_{k=2}^{n} A_k \sin\varphi_k(t) + n(t) \quad \ldots \tag{7}$$

$$where \varphi_k(t) = \omega_k t + \varphi_k$$

is the total phase angle of the kth constituting component called $r_k(t)$, and $n(t)$ denotes the total noise imposed on the signal. The first component called the fundamental component is deliberately signaled out in (1) due to its significance in power signals. The signals attribute A_k, ω_k and φ_k are magnitudes, frequencies and phase angles of the constituting components and can be time-varying. The noise n(t) is assumed as a zero-mean white Gaussain noise with a variance of σ^2. The kth component is primarily specified by its amplitude A_k and its frequency ω_k but its instantaneous value $A_k \sin\varphi_k(t)$ can also be of interest in some applications. The APF technique is a structure composed of n-coupled parallel filters so that each one extracts a component of the power signal and estimates its frequency. The dynamic

behavior of the algorithm is characterized by the following set of differential equations as in [29]:

$$\ddot{x}_k(t) = -\theta_k^2(t)x_k(t) + 2\varsigma_k\theta_k(t)e(t)$$

$$\dot{\theta}_k(t) = -\gamma_k x_k(t)\theta_k(t)e(t), \qquad \ldots \qquad (8)$$

$$k = 1,\ldots,n$$

$$e(t) = r(t) - \sum_{k=1}^{n}\dot{x}_k(t)$$

where the dot sign is used to denote the time derivative. In (2), θ_k is the estimated frequency (in radians per second) of the kth component, ς_k and γ_k are the real positive numbers which are the design parameters of the kth subfilter and it determines its behavior in terms of accuracy (steady state) and convergence speed (transient). The normalized γ_k is used to remove the dependency of the averaged system to amplitude as given below

$$\gamma_k = \frac{\gamma_0}{\mu + N(x_k^2\theta_k^2 + \dot{x}_k^2)} \qquad (9)$$

where $\gamma_0 = \alpha N$, $\zeta_k = \varsigma_0/k^2$, μ and N are real positive constants. The constant μ is a small positive constant to prevent the denominator of γ_k from becoming zero. The two design parameters α and ς_0 determines the dynamical behavior of the whole algorithm in terms of the transient and steady-state responses.

The block diagram of the filter is shown in Fig.1. The dynamic system (2) for the input signal (1) with $\varphi_k(t) = \omega_k t + \varphi_k$ and $n(t) = 0$ has a unique quasi periodic orbit given by

$$P(t) = (P_1^T(t)\ldots P_n^T(t))^T \qquad \ldots \qquad (10)$$

where $P_k(t)$ is given by

$$P_k(t) = \begin{pmatrix} \bar{x}_k \\ \dot{\bar{x}} \\ \bar{\theta}_k \end{pmatrix} = \begin{pmatrix} -\dfrac{A_k}{\omega_k}\cos\varphi_k(t) \\ A_k\sin\varphi_k(t) \\ \omega_k \end{pmatrix} \qquad \ldots \qquad (11)$$

$$k = 1,\ldots,n$$

This represents that the kth constituting component of the input signal as well as its frequency are directly provided by the kth set of the differential equations, and hence a full set of decomposition is achieved if a sufficient number of filters are

employed. The structural block diagram of the algorithm is shown in Fig.1 in which the detailed implementation block diagram of the *k*th subfilter is shown. The error signal e(t) is applied to each subfilter, and the θ_k update law of (2) is employed to force the error signal to zero. This enables each subfilter to focus on a component and extract it. Each subfilter is not fixed at any specific components. The initial value of the integrator of the frequency update law in (2) is set to θ_{k0}, which is equal to the nominal value of the frequency of the *k*th component to be extracted.

The amplitude and the phase of kth component of the input signal is

$$\left(\overline{\theta}_k^2 \overline{x}_k^{-2} + \overline{\dot{x}}_k^{-2}\right)^{1/2} = A_k$$

$$\varphi_k(t) = \begin{cases} \arccos\left(\dfrac{-\theta_k x_k}{A_k}\right) ; \dot{x}_k \succ 0 \\[4mm] 2\pi - \arccos\left(\dfrac{-\theta_k x_k}{A_k}\right) ; \dot{x}_k \prec 0 \end{cases} \quad \dots \quad (12)$$

Thus the ANF estimates harmonics and interharmonics as shown in the Fig.1 with five subfilters.
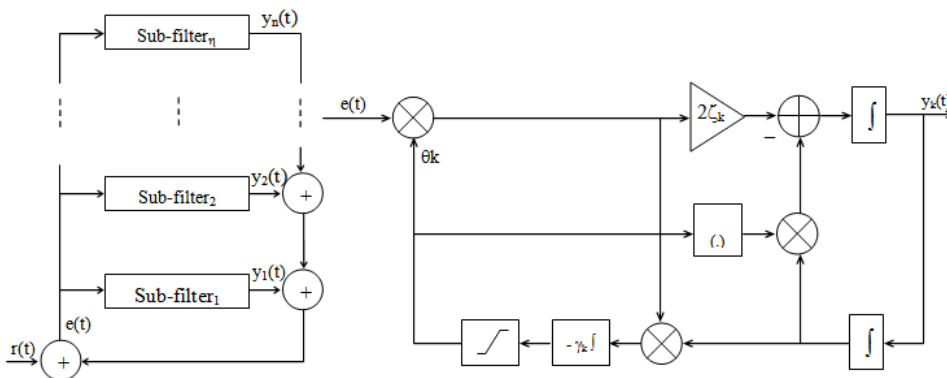
Figure 1: Block diagram representation of the frequency estimator and the detailed representation of the kth paralleled subfilter.

Results and Discussions

Different power system events are considered and their event tracking using Time-frequency methods using LabVIEW and Adaptive comb-peak filters uing Matlab/simulink are discussed with synthetic signals in which f represents frequency in Hz, A represents amplitude and t represents time in seconds.

Voltage Swell at 0.1-0.2s
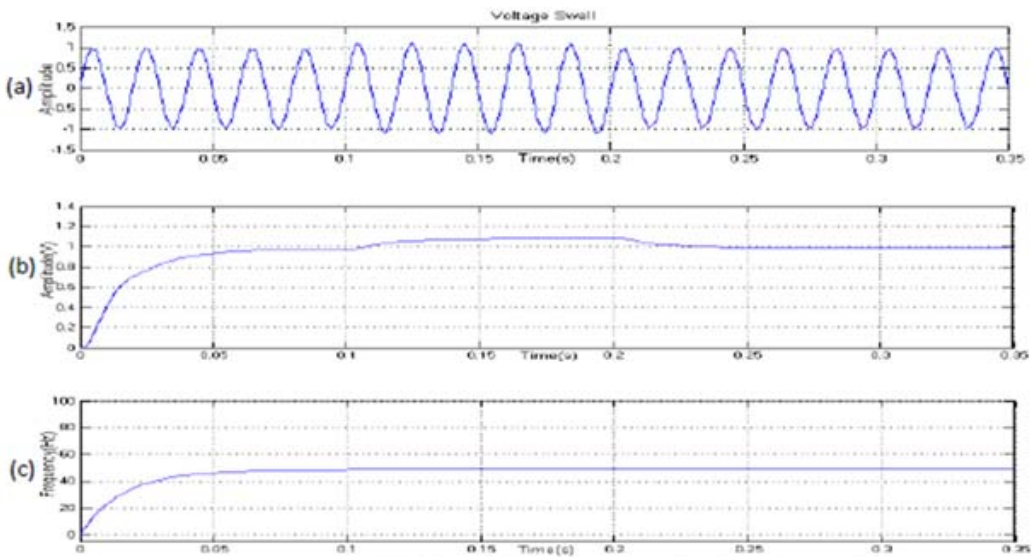A 10% voltage swell begins at t = 0.1s and ends at 0.2s. The test voltage waveform

sampled at the rate of 1000Hz with f = 50Hz and A=1, is shown in Fig.2(a)
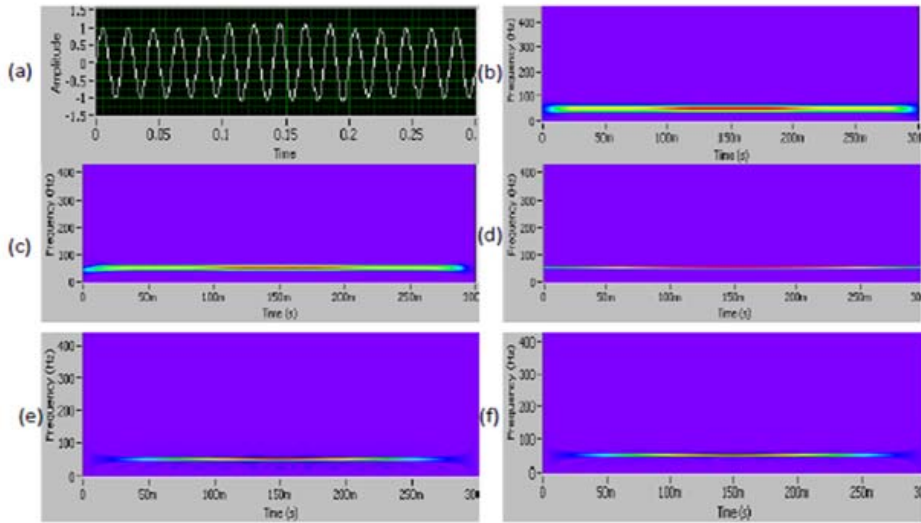
Figure 2: TF analysis of Voltage swells (a) Input signal (b) STFT (c) Gabor spectrogram (d) Adaptive Spectrogram (e) WVD (f) CWD

The adaptive spectrogram gives the best frequency resolution, but there is poor time information. It is blurred and has inaccurate time information, as shown in Fig.2(d). The WVD and CWD gives better time and frequency resolution. The STFT and Gabor give better time resolution. The deep red part, starting at 1s, indicates the higher voltage level than the nominal voltage, identifying the PQ event as a voltage swell.

Figure 3: ACF analysis of Voltage swells (a) Input signal (b) Estimated Amplitude

(c) Estimated Frequency

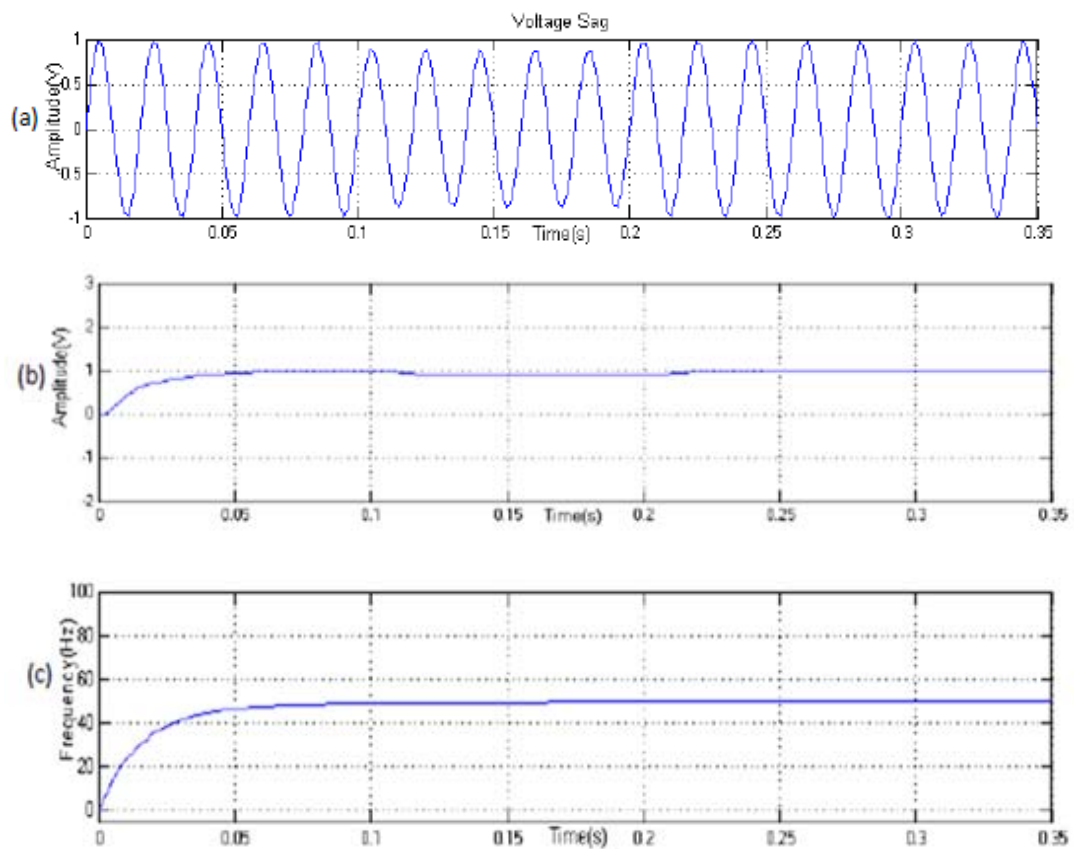The increase in the amplitude at 0.1s is clearly estimated and tracked as shown is Fig.3(b) and frequency in Fig.3 (c)

Voltage Sag at 0.1-0.2s
A 10% voltage sag begins at t=0.1s and ends at 0.2s. The test voltage waveform sampled at the rate of 1000Hz with f=50Hz and A=1, is shown in Fig.4(a)
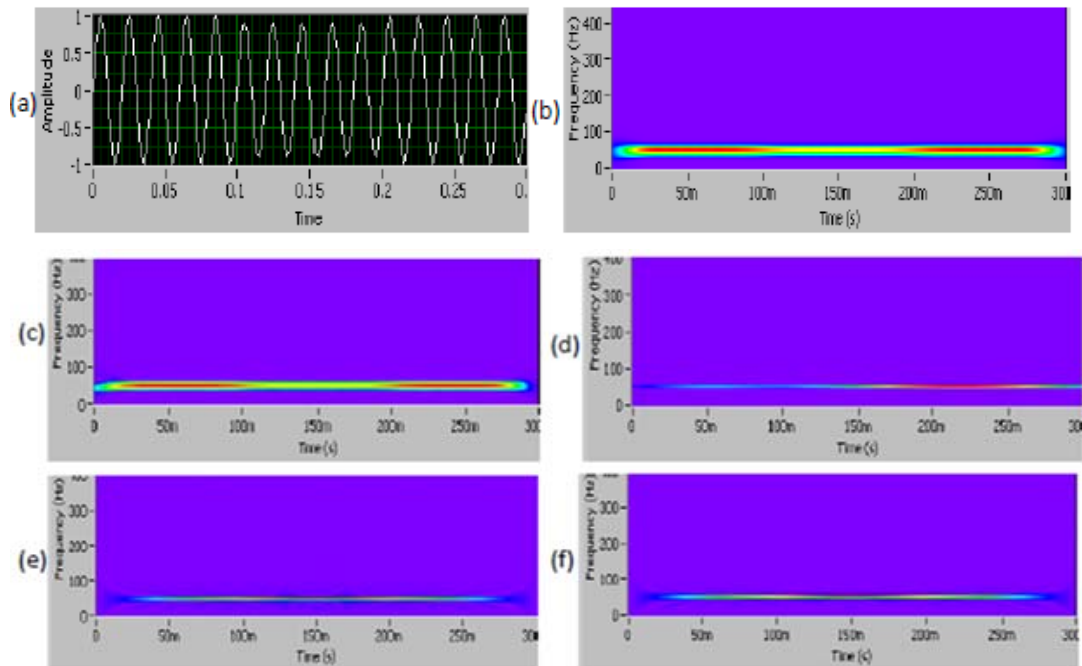
Figure 4: TF analysis of Voltage sag (a) Input signal (b) STFT (c) Gabor spectrogram (d) Adaptive Spectrogram (e) WVD (f) CWD

The STFT and Gabor give poor time and frequency resolution, as shown in Fig.4(b), 4(c). The WVD and CWD give better time and frequency resolution. The deep red part, starting at 1s, indicates the higher voltage level than the nominal voltage, identifying the PQ event as voltage sag.

Figure 5: ACF analysis of Voltage sags (a) Input signal (b) Estimated Amplitude (c) Estimated Frequency

The decrease in the amplitude at 0.1s is clearly estimated and tracked as shown in Fig.5(b). Frequency of the power signal is shown in Fig.5(c).

**Harmonics/Intreharmonics 50,150,210 Hz**
A voltage signal in which a fundamental f1 = 50Hz, amplitude A=1, third harmonic of f3 = 150Hz, A3 = 0.8 and an interharmonic of f4=210Hz, A4=0.6 are added as shown in Fig.6(a).
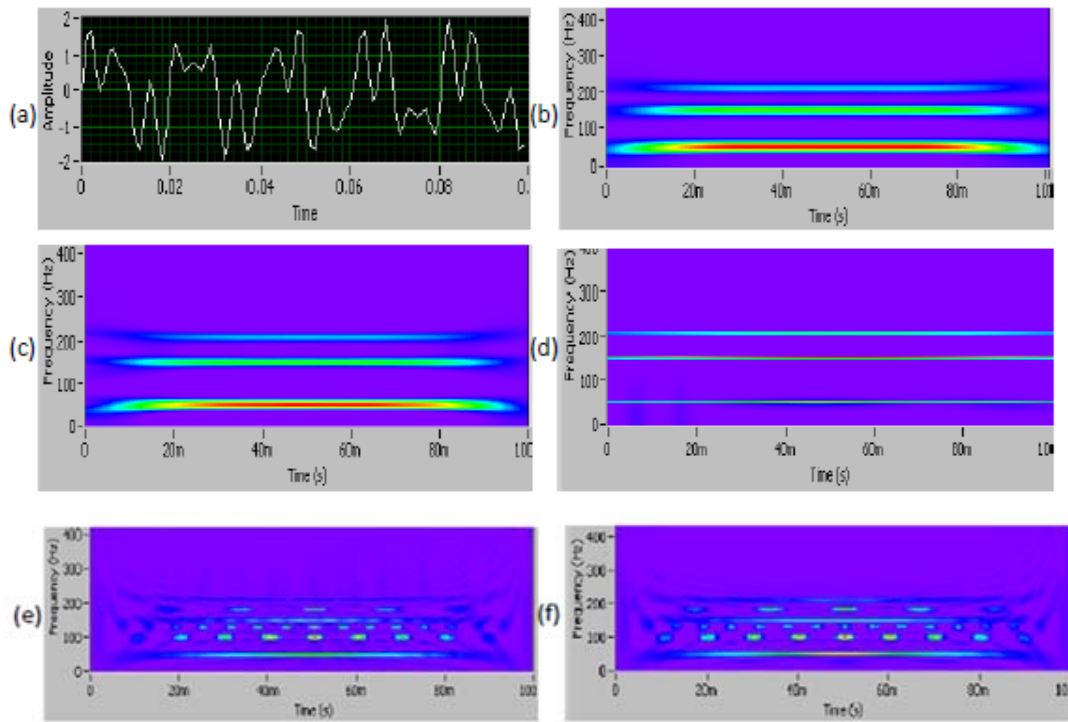
Figure 6: TF analysis of harmonics/interharmonics (a) Input signal (b) STFT (c) Gabor spectrogram (d) Adaptive Spectrogram (e) WVD (f) CWD

The adaptive spectrogram gives the better time and frequency resolution, as shown in Fig.6(d) the CWD gives better frequency resolution but both WVD and CWD includes crossterms. The STFT and Gabor provides poor frequency resolution.
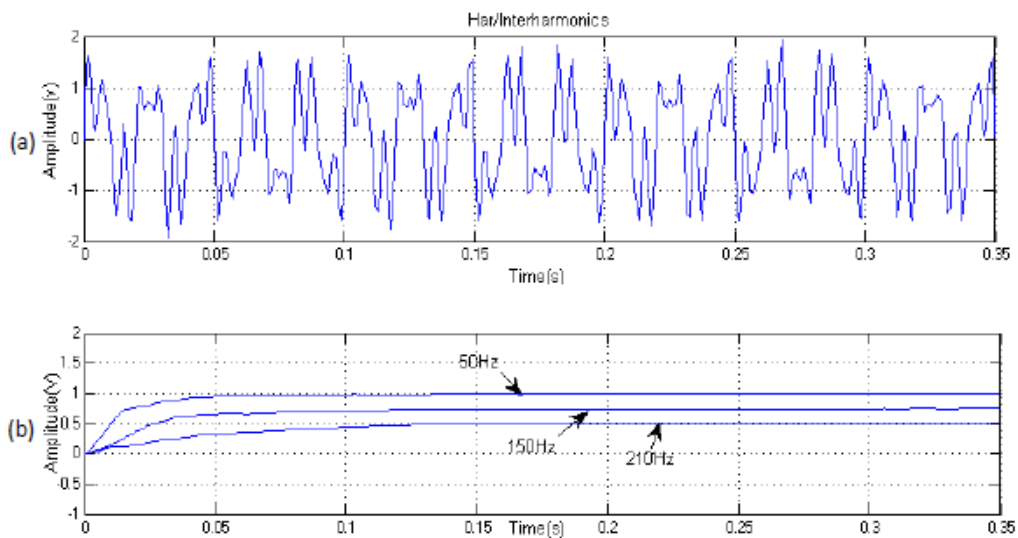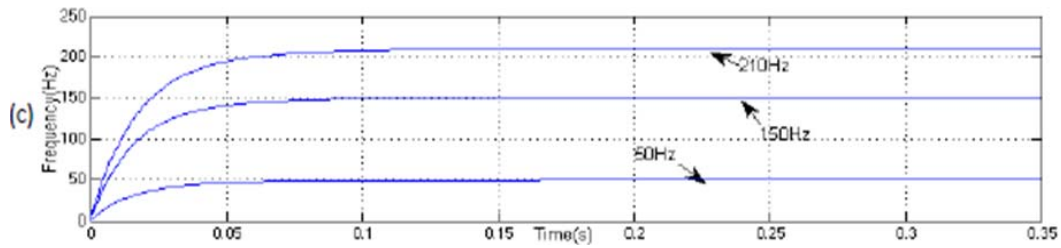
Figure 7: ACF analysis of harmonics/interharmonics (a) Input signal (b) Estimated Amplitude (c) Estimated Frequency

By arranging three filters in parallel each estimates individual harmonics/interharmonics separately. Fig.7(b), 7(c) shows the estimated amplitude and frequency respectively.
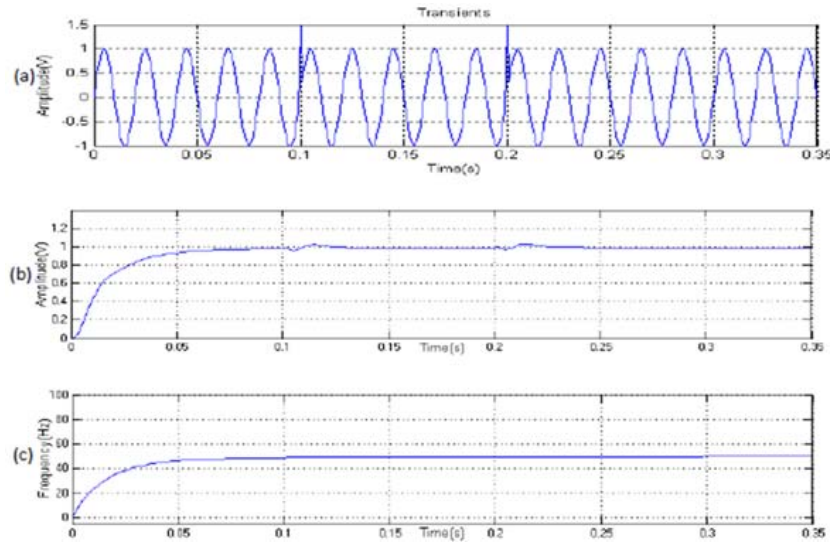
Transients at 0.1 & 0.2s

A voltage signal containing two transient event at 0.1s and 0.2s of 1.5 amplitude is shown in Fig.8(a).
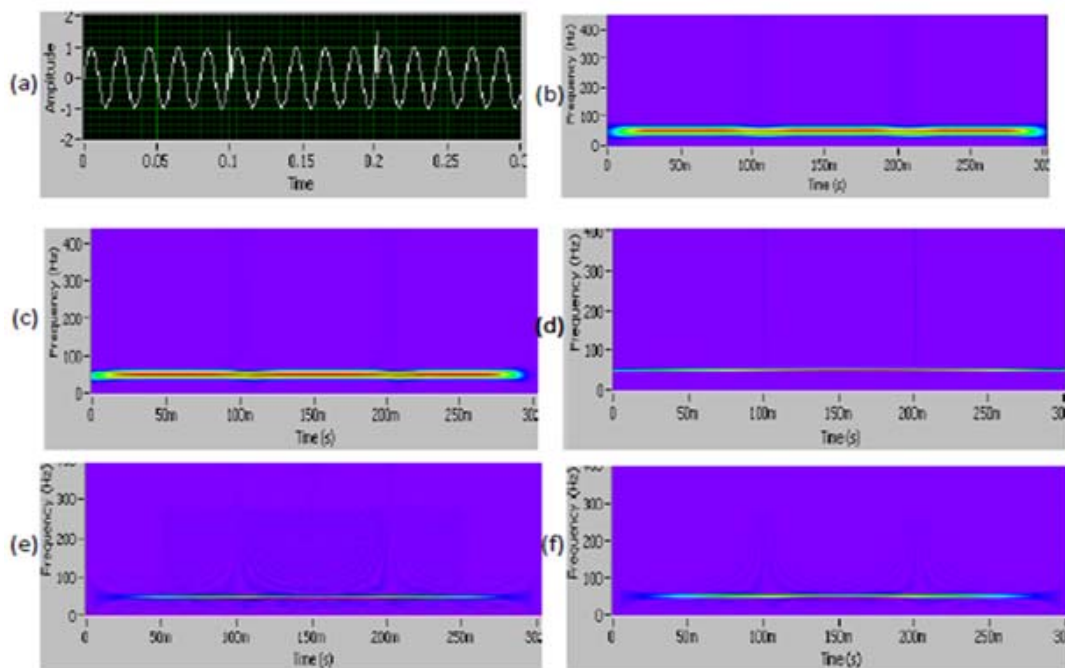
Figure 8: TF analysis of transients (a) Input signal (b) STFT (c) Gabor spectrogram (d) Adaptive Spectrogram (e) WVD (f) CWD

The STFT and Gabor transform as shown in Fig.8(b), 8(c) detects the transients but other methods are not able to show the transient event.

Figure 9: ACF analysis of transients (a) Input signal (b) Estimated Amplitude (c) Estimated Frequency

The transient events are detected accurately at 0.1s and 0.2s in the estimated amplitude as shown in Fig.9(b)

Flickering at 0.1s 50+20Hz
A voltage signal with voltage fluctuation, also known as flicker, begins at 0.1s. The 50Hz signal added with 20Hz low frequency component as shown in Fig.10(a).
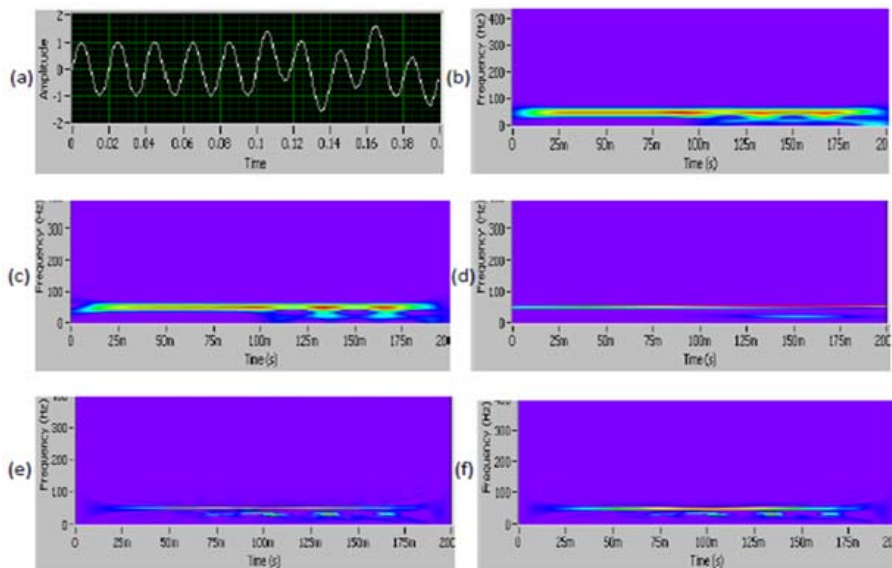
Figure 10: TF analysis of Voltage flicker (a) Input signal (b) STFT (c) Gabor spectrogram (d) Adaptive Spectrogram (e) WVD (f) CWD

The adaptive spectrogram gives better results in case of flicker when the other methods do not show the low frequency component as shown in Fig.10(d).
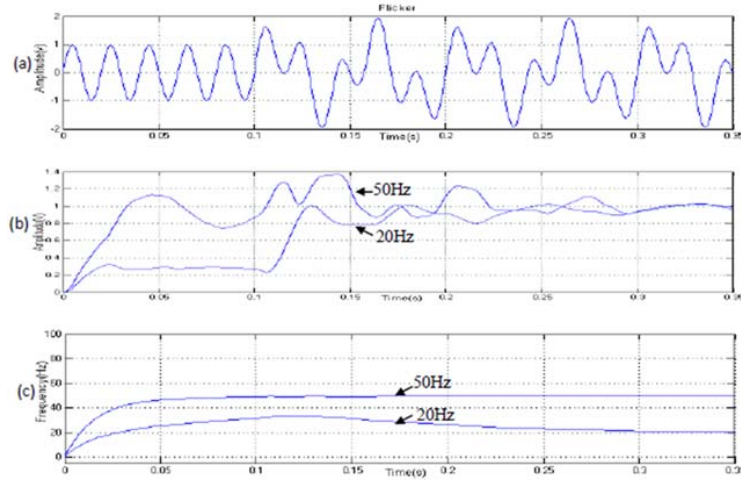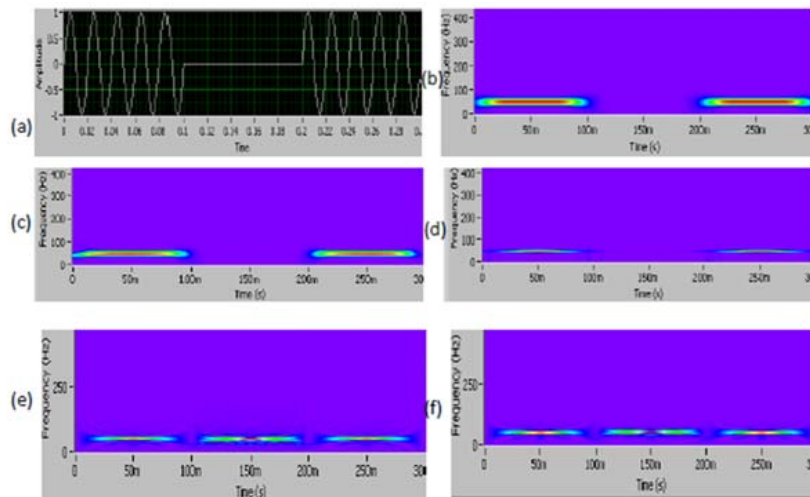

Figure 11: ACF analysis of Voltage flicker (a) Input signal (b) Estimated Amplitude (c) Estimated Frequency

The low frequency component occurring at 0.1s is detected in the estimated frequency as shown in Fig.11(c) but the amplitude of the signal takes more time to settle.
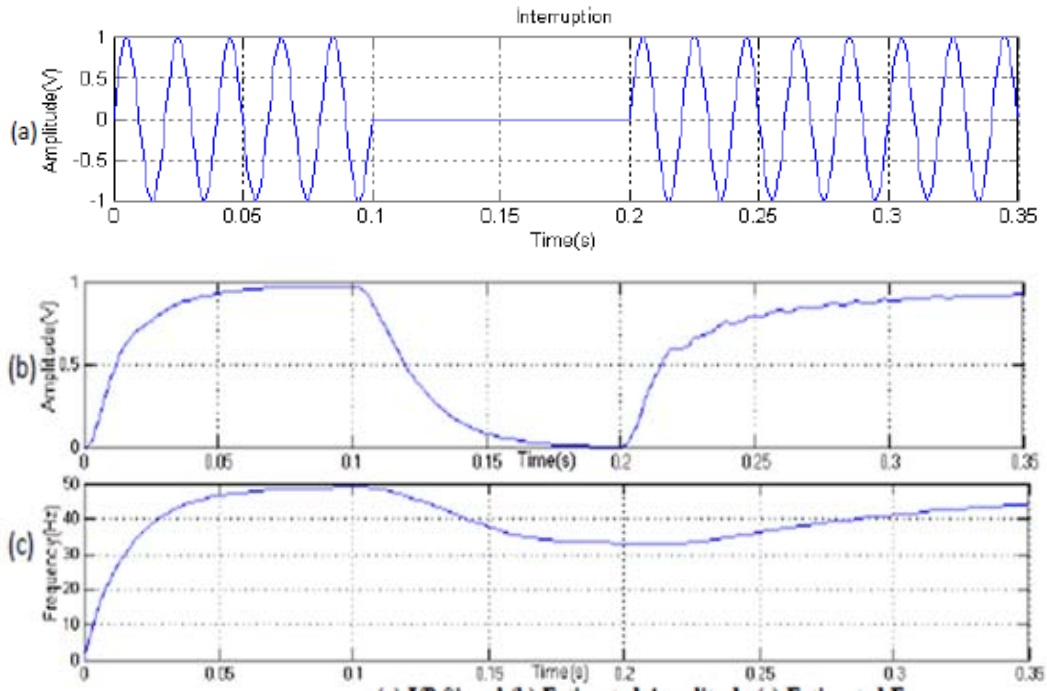
Interruption at 0.1-0.2s
Voltage signal is absent in 0.1s to 0.2s as shown in Fig.12(a).

Figure 12: TF analysis of Voltage interruption (a) Input signal (b) STFT (c) Gabor spectrogram (d) Adaptive Spectrogram (e) WVD (f) CWD

The adaptive spectrogram gives the better time and frequency resolution, as shown in Fig.12(d). The CWD gives the better frequency resolution but both WVD and CWD includes crossterms. The STFT (Fig.12(b)) and Gabor (Fig.12(c)) gives poor frequency resolution.

Figure 13: ACF analysis of Voltage interruption (a) Input signal (b) Estimated Amplitude (c) Estimated Frequency

The decrease in amplitude at 0.1s and approaches towards zero indicates interruption occurs as shown in Fig.13(b) and Fig.13(c)

Frequency Variation at 0.1s 50-60Hz
Voltage signal with multi frequencies, whose frequency changes from 50 to 60Hz at 0.1s is analyzed as shown in Fig.14(a). The frequency variation is accurately tracked as shown in Fig.14 (c)
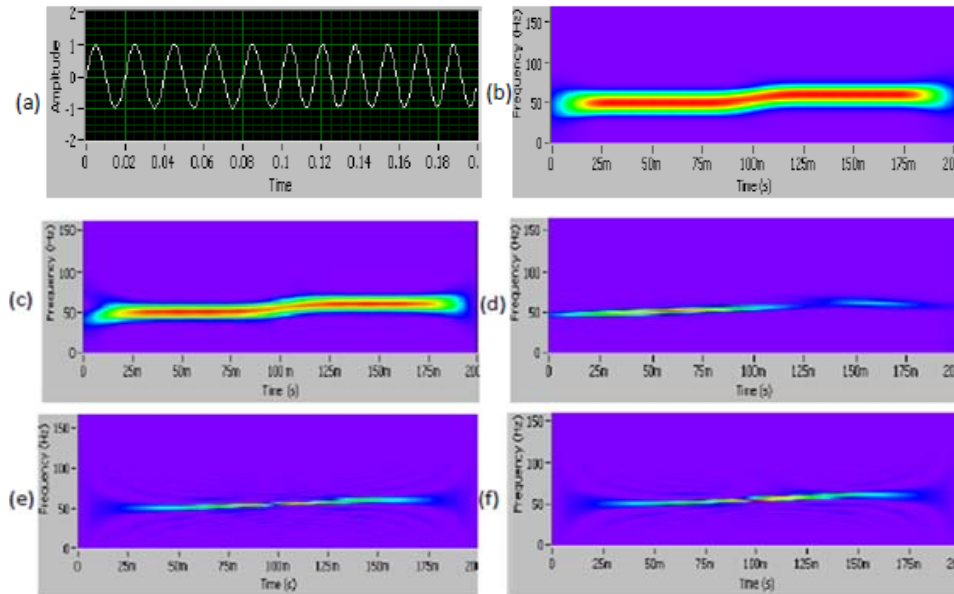
Figure 14: TF analysis of frequency variations (a) Input signal (b) STFT (c) Gabor spectrogram (d) Adaptive Spectrogram (e) WVD (f) CWD

The WVD (Fig.14(e)) and CWD (Fig.14(f)) gives better variation with both time and frequency resolution. STFT (Fig.14(b)) and Gabor shows poor frequency resolution.
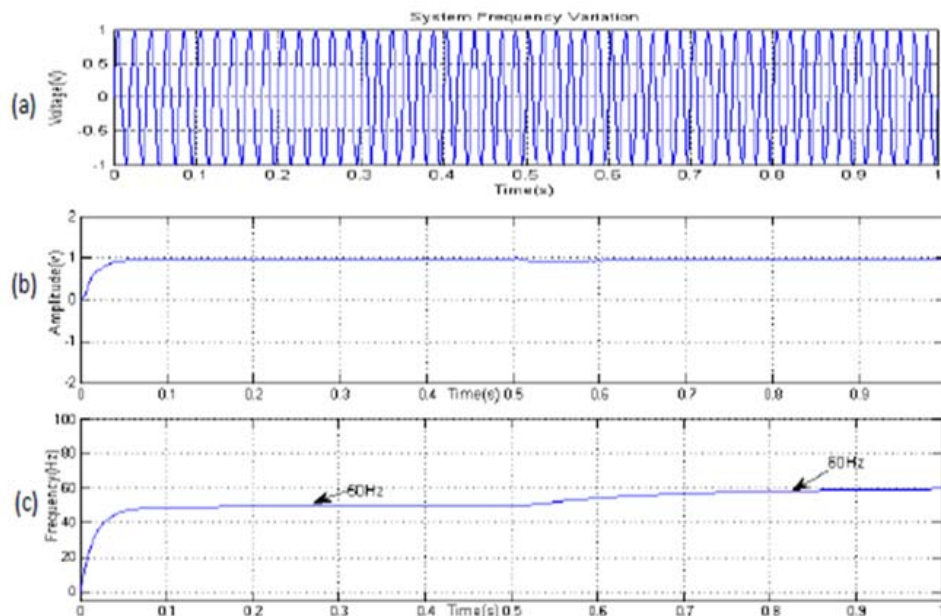
Figure 15: ACF analysis of frequency variations (a) Input signal (b) Estimated Amplitude (c) Estimated Frequency

The change in frequency can be seen in Fig.15(c). The Table.1 discusses the difference in the detection of power quality disturbances using time-frequency analysis and adaptive comb-peak filters, which conclude that the change in frequency and amplitude is detected using Adaptive comb filter accurately.

Table 1: Performance analysis using TFA and ACF for different power system events

Events	STFT	Gabor	Adaptive Spectrogram	WVD	CWD	ACF
Swell	Poor frequency resolution	Poor frequency resolution	Poor time resolution	Better	Better	Detects
Sag	Poor frequency Resolution	Poor frequency resolution	Poor time resolution	Better	Better	Detects
Harmonics/ Interharmonics	Poor frequency resolution	Poor frequency Resolution	Better	Includes crossterms	Includes Crossterms	Detects
Transients	Detects	Detects	Poor detection	Poor detection	Poor detection	Detects
Flicker	Poor frequency Resolution	Poor frequency Resolution	Better	Poor frequency Resolution	Poor frequency Resolution	Detects
Interruption	Poor frequency Resolution	Poor frequency Resolution	Better	Includes crossterms	Includes crossterms	Detects
System frequency variation	Poor frequency Resolution	Poor frequency Resolution	Better	Better	Better	Detects

Conclusion

The Time-Frequency domain based methods of monitoring the power system disturbances are not giving the accurate values of the signal amplitude and frequency. It is difficult to choose the single method to analyze all power system disturbances. The adaptive comb filter method gives accurate values and also easy in implementation. The analysis shows that the adaptive comb filter gives best performances in all power system disturbances compared to Time-Frequency analysis. One limitation is the selection of the number of sub filters for analysis. These Sub filters provide a single component value at a time, which requires the knowledge about the frequency content of the signal.

References

[1] J. Arrillaga and Neville R. Waston, *Power System Harmonics,* Second Edition, John Wiley & Sons Ltd, 2003.

[2] V. Baghzouz, R.F. Burch, A. Capasso, A. Cavallini, A. E. Emanuel, M. Halpin, A. Imece, A. Ludbrook, G. Montanari, K.J. Olejniczak, P. Riberio, S. Rios-Marcuello, L.Tang, R. Thallam, P. Verde, "Time-varying harmonics: Part I—Characterizing measured data," *IEEE Trans. Power Del.,* vol. 13, no. 3, pp. 938–944, Jul. 1998.

[3] A.Testa, M.F. Akram, R. Burch, G. Carpinelli, G. Chang, V. Dinavahi, C. Hatziadoniu, W.M. Grady, E. Gunther, M. Halpin, P. Lehn, Y. Liu, R. Langella, M. Lowenstein, A. Medina, T. Ortmeyer, S. Ranade, P. Riberio, N. Watson, J. Wikston, and W.Xu, "Interharmonics: Theory and Modeling, IEEE Task Force on Harmonics Modeling and Simulation", *IEEE Trans on Power Delivery*, vol. 22, no. 4, pp.2335-2348, Oct. 2007.

[4] Cheng-I Chen, Gary W.Chang, "Virtual instrumentation and educational platform for time-varying , harmonic and interharmonic detection", *IEEE Trans. on Industrial Electronics*, vol. 57, no.10, pp.3334-3342, Oct 2010.

[5] Math H.J.Bollen, Irene Y.H. Gu, Surya Santoso, Mark F. McGranaghan, Peter A.Gossley, Moises V. Riberio and Paulo F. Ribeiro, "Assessing power system quality using signal processing techniques", *IEEE Signal Processing magazine*, pp.12-31, July 2009.

[6] A. A. Girgis and F. M. Ham, "A qualitative study of pitfalls in FFT," *IEEE Trans. Aerosp. Electron. Syst.*, vol. AES-16, pp. 434–439, July 1980.

[7] T. A. George and D. Bones, "Harmonic power flow determination using the fast Fourier transform," *IEEE Trans. Power Del.*, vol. 6, no. 2, pp. 530–535, Apr. 1991.

[8] D. Gabor, "Theory of Communications," *Journal of IEEE (London)*, vol.93, no. III, pp. 429- 457, 1996.

[9] V. L. Pham and K. P. Wong, "Wavelet-transform-based algorithm for harmonic analysis of power system waveforms," *Proc. Inst. Electr. Eng.—Gener. Transm. Distrib.*, vol. 146, no. 3, pp. 249–254, May 1999.

[10] E. Y. Hamid and Z. Kawasaki, "Wavelet packet transform for rms values and power measurements," *IEEE Power Eng. Rev.*, vol. 21, no. 9, pp. 49– 51, Sep. 2001.

[11] T. Tarasiuk, "Hybrid wavelet-Fourier spectrum analysis," *IEEE Trans.Power Del.*, vol. 19, no. 3, pp. 957–964, Jul. 2004.

[12] J. Barros and R. I. Diego, "Application of the wavelet packet transform to the estimation of harmonic groups in current and voltage waveforms," *IEEE Trans. Power Delivery*, no. 1, vol. 21, pp. 533-535, January 2006.

[13] Walid G. Morsi and M. E. El-Hawary, "Suitable Mother Wavelet for Harmonics and Inter- Harmonics Measurements Using Wavelet Packet Transform" in *Proc. Canadian Conference of Electrical and Computer Engineering, 2007, CCECE 2007*, pp. 748-752, Apr. 2007.

[14]   A. A. Girgis, W. B. Chang, and E. B. Makram, "A digital recursive measurement scheme for on-line tracking of power system harmonics," *IEEE Trans. Power Del.*, vol. 6, no. 3, pp. 1153–1160, Jul. 1991.

[15]   M. Bettayeb and U. Qidwai, "Recursive estimation of power system harmonics," *Elect. Power Syst. Res.*, vol. 47, no. 2, pp. 143–152, Oct. 1998.

[16]   Li Tan, Jean Jiang, "Novel adaptive IIR filter for frequency estimation and tracking", *IEEE Signal Processing Magazine*, pp.186-189, Nov-2009.

[17]   Monson H. Hayes, John Treichler, "Adaptive filtering", IEEE Signal Processing Magazine, pp.169-172, Nov.2008

[18]   J. F. Chicharo and H.Wang, "Power system harmonic signal estimation and retrieval for active power filter applications," *IEEE Trans. Power Electron.*, vol. 9, no. 6, pp. 580–586, Nov. 1994.

[19]   P. A. Regalia, "An improved lattice-based IIR notch filter," *IEEE Trans.Signal Process.,   vol. 39, no. 9, pp. 2124–2128, Sep. 1991.*

[20]   I. Kamwa and R. Grondin, "Fast adaptive schemes for tracking voltage phasor and local frequency in power transmission and distribution systems," *IEEE Trans. Power Del.*, vol. 7,no. 2, pp. 789–795, Apr. 1992.

[21]   C. S. Moo, Y. N. Chang, and P. P. Mok, "A digital measurement scheme for time-varying transient harmonics," *IEEE Trans. Power Del.*, vol. 10, no. 2, pp. 588–594, Apr. 1995.

[22]   P. K. Dash, D. P. Swain, A. C. Liew, and S. Rahamn, "An adaptive linear combiner for on-line tracking of power system harmonics," *IEEE Trans. Power Syst.*, vol. 11, no. 4,   pp. 1730–1735, Nov. 1996.

[23]   L. L. Lai, C. T. Tse, W. L. Chan, and A. T. P. So, "Real-time frequency and harmonic evaluation using artificial neural networks," *IEEE Trans. Power Del.*, vol. 14, no. 1, pp. 52–59, Jan. 1999.

[24]   M. Karimi-Ghartemani and M. R. Iravani, "A nonlinear adaptive filter for on-line signal analysis in power systems: Applications," *IEEE Trans. Power Delivery*, vol. 17, no. 2, pp. 617–622, Apr. 2002.

[25]   M. Bodson, Scott C. Douglas, "Adaptive algorithms for the rejection of sinusoidal disturbances with unknown frequency," *Automatica, vol.*33, no. 12, pp. 2213–2221, 1997.

[26]   M. Karimi-Ghartemani and A. K. Ziarani, "Periodic orbit analysis of two dynamical systems for electrical engineering applications," *J. Eng. Math.*, vol. 45, no. 2, pp. 135–154, Feb. 2003

[27]   M. Mojiri, M. Karimi-Ghartemani, and A. R. Bakhshai, "Time-domain signal analysis using adaptive notch filter," *IEEE Trans. Signal Process.*, vol. 55, no. 1, pp. 85–93, Jan. 2007.

[28]   M. Mojiri and A. R. Bakhshai, "Estimation of n frequencies using adaptive notch filter," *IEEE Trans. Circiuts Syst. II*, vol. 54, no. 4, pp.338–342, Apr. 2007.

[29]   Mohsen Mojiri, Masoud Karimi-Ghartumani, Alireza Bakhshai, "Processing of Harmonics and Interharmonics Using an Adaptive Notch Filter," IEEE *Transactions On Power Delivery, Vol. 25, No. 2, April 2010.*

[30] Davood Yazdani, Alireza Bakhshai, Praveen K. Jain, "A three phase based approach to harmonic/reactive current extraction and harmonic decomposition", IEEE Trans. on Power Electronics, vol.25, no.4, April 2010, pp.914-923.

[31] Jason Levin, Nestor O. Perez, Arancibia, Petros A. Joannou, "Adaptive notch filter using real-time parameter estimation", IEEE Trans. on Control System Technology, early access.

[32] M. Mojiri, A.R. Bakhshai, "Estimation of n Frequencies using Adaptive Notch Filter", IEEE Trans. on Circuits & Systems II : Express briefs, vol.54, no.4, April 2007, pp.338-342.

[33] Maurizio Cirrincione, Marcello Pucci, Gianpuolo Vitale, Abdellatif Miraoui, "Current harmonic compensation by a single phase shunt active power filter by adaptive notch filter", IEEE Trans. on Industrial Electronics, vol.56, no.8, pp.3128-3143, Aug.2009.

[34] M. Karimi-Ghartemani and M. R. Iravani, "Measurement of harmonics/ inter-harmonics of time-varying frequencies," *IEEE Trans. Power Del.*, vol. 20, no. 1, pp. 23–31, Jan. 2005.

[35] Hugh Douglas, Pragasen Pillay, Alireza K. Ziarani, "A new algorithm for transient motor current signature analysis using wavelets", IEEE Trans. on Industry Applications, vol.40, no.5, Sep/Oct 2004, pp.1361-1367

[36] Janison Rodrigues de Carvalho, Carlos A. Duque, Moises V. Ribeiro, Augusto S. Cerqueira, Thomas L. Baldwin, Paulo F. Ribeiro, "A PLL-based multirate structure for time-varying power systems harmonic/Interharmonic estimation", IEEE Trans. on Power Delivery, vol.24, no.4, Oct 2009, pp.1789-1800.

[37] Dragon S. Maric, Silva Hiti, Constantin C. Stancu, James M. Nagashimma, David B. Rutledge, "An application of a constrained adaptive lattice-structure all-pass based notch filter for advanced control of surface mounted permanent magnet synchronous drive", IEEE Trans. on Circuits and Systems I: fundamental theory and applications, vol.46, no.12, pp. 1513-1516, Dec.1999.

[38] Serkan Gunal, Dogan Gokhan Ece, Omer Nezih Gerek, "Induction motor condition monitoring using notch filtered motor current", Mechanical Systems and Signal Processing 23(2009), 2658-2670.

[39] Satish Rajagopalan, JosenA. Restrepo, Jose M.Aller, Thomas G. Habetler, Ronald G. Harley, "Nonstationary motor fault detection using recent quadratic time-frequency representations", IEEE Trans. on Industry applications, vol.44, no.3, May/June 2008.

[40] A.R. Abdullah, A.Z. Sha'ameri, and N.M.Saad, "Power quality analysis using spectrogram and Gabor transformation," in Proc. Asia Pacific Conf. Applied Electromag., Melaka, Malaysia, Dec. 4-6, 2007, pp. 1-5.

[41] Soo-Hwan Cho, Gilsoo Jang, "Time-Frequency Analysis of power-Quality Disturbances via the Gabor-Wigner Transform," IEEE Trans. on Power Delivery, vol.25, no.1, Jan 2010.

[42] S. Qian and D. Chen, "Discrete Gabor Transform," IEEE Trans. on Signal Process, vol.41, no.7, pp.2429-2438, Jul.1993.